CH4 dissociation on Ni(100): Comparison of a direct dynamical model to molecular beam experiments

Luntz, Alan

Published in:
Journal of Chemical Physics

Link to article, DOI:
10.1063/1.468956

Publication date:
1995

Document Version
Publisher's PDF, also known as Version of record

CH_4 dissociation on Ni(100): Comparison of a direct dynamical model to molecular beam experiments

A. C. Luntz[a)]
Physics Department, Technical University of Denmark, DK-2800 Lyngby, Denmark

(Received 24 October 1994; accepted 16 February 1995)

This paper makes an extensive comparison of a dynamical model for a mechanism of direct dissociation to the detailed molecular beam experiments of CH_4 dissociation on a Ni(100) surface reported in the previous paper. When a PES incorporating an ''exit channel'' barrier is used in the model and steric (multidimensional) aspects are included approximately via a ''hole'' approximation, excellent agreement is achieved between the model and experiments. This strengthens the qualitative mechanistic conclusions of Holmblad, Wambach, and Chorkendorff [J. Chem. Phys. **102**, 8255 (1995)]. © *1995 American Institute of Physics.*

I. INTRODUCTION

A mechanistic discussion of the dissociation of small alkanes on metal surfaces has been an extremely active (and controversial) area within surface science over the past two decades because of its importance in industrial catalysis. No system is perhaps more important in this regard than the dissociation of CH_4 on Ni(100) since this is the best single crystal model for the rate limiting step in the commercial process of steam reforming of natural gas. The previous paper,[1] hereafter referred to as I, presents detailed molecular beam experiments for the dissociation of CH_4 on a Ni(100) surface. These experiments show a very strong dependence of the bare surface dissociation probability S_0 on CH_4 incident normal energy E_n and CH_4 vibrational (i.e., nozzle) temperature T_v. Moderate, but still significant dependences of S_0 on isotope and surface temperature T_s are also observed. All dependencies on the various experimental parameters are strongly coupled; e.g., the dependence on T_v depends on E_n, the dependence on E_n depends on T_v, the dependence on T_s depends on both E_n and T_v, etc.

The authors of Paper I argue that many of their results are qualitatively consistent with a direct dissociation mechanism on a potential energy surface (PES) with an ''exit channel'' barrier, i.e., principally along a C–H vibrational coordinate. They fit the observed dependence of S_0 on E_n and T_v to empirical ''S''-shaped excitation functions, one for each of the three lowest vibrational states of a quasidiatomic R–H molecule. Although this provides a very good fit to the data and a reasonable rationale for the strong dependence on both E_n and T_v, the empirical S excitation functions are not fully consistent with two dimensional dynamics since the energy separation between the S functions is more than the vibrational energy ω_{vib}.

Luntz and Harris[2] have previously discussed in some detail a dynamical model for a mechanism of direct alkane dissociation on transition metal surfaces. This model is based on solving for the direct dissociation dynamics quantum mechanically on a reasonable reduced dimensionality PES for a quasidiatomic R–H interacting with a dynamic metal surface. With a PES where the barrier was largely entrance channel dominated, reasonable qualitative agreement was obtained between the model and molecular beam experiments for the dissociation of CH_4 on Pt(111), as well as with a variety of other molecular beam and thermal experiments.[2]

In this paper, the reduced dimensionality dynamical model is developed for a PES with an exit channel barrier. In addition, steric factors (multidimensionality) are accounted for statically via the so-called ''hole'' approximation.[3,4] The resulting model shows excellent agreement with the molecular beam experiments of Paper I, and easily rationalizes the large separation between the empirical S functions utilized to fit the data.

II. DYNAMICAL MODEL

In the dynamical model of Luntz and Harris,[2] quantum dynamics on an assumed PES $V(Z,D,Y)$ describes a mechanism of direct dissociative chemisorption of a quasidiatomic R–H on a metal surface. Z, D, and Y are the translational, vibrational, and a surface phonon (cube) coordinate, respectively. The dependence of the dissociation reaction coordinate on all three then rationalizes in a simple way the dependence of S_0 on E_n, T_v, and T_s and a strong coupling between the experimental dependences.

In the original presentation of this model,[2,5] the importance of tunneling was emphasized by the authors. This has regrettably caused considerable confusion as to the essential aspect of the model, i.e., that it is a reduced dimensionality dynamical model for the mechanism of direct dissociation. Tunneling is in no way required by the mechanism nor for the model to be valid, and this has been pointed out briefly in subsequent discussions and applications of the model.[6,7] The dependence of the reaction dynamics on all three coordinates Z, D, and Y occurs whether tunneling is important or not. The nuclear dynamics describing dissociation on the assumed PES is solved quantum mechanically so that if tunneling is important in the dynamics it is included automatically. However, the quantum solution of the dissociation dynamics in no way forces tunneling to be important. This is strictly a function of the assumed PES, e.g., the width of the barrier and the initial conditions, e.g., E_n. For the PES assumed here, tunneling is important in the reduced dimension-

a)Present address: IBM Research, Almaden Research Laboratory, 650 Harry Rd., San Jose, CA 95120.

 0021-9606/95/102(20)/8264/6/$6.00

ality dynamical model under some initial conditions (low E_n and T_v) and unimportant at others (high E_n and T_v). While it is straightforward in the reduced dimensionality model to determine when tunneling is important, this is a considerably more subtle issue in full dimensionality dynamical models of dissociation (and hence in the experimental world). In this case, there is a wide distribution of barriers due to ''steric'' factors. A given incident energy can then be either above the barrier for some steric conditions (orientation, impact parameter, etc.) and below the barrier for other steric conditions. Since the dissociation probability also depends on the distribution of barriers, it is difficult to decide in a multidimensional world if tunneling is in fact dominant under many given experimental conditions. Since tunneling is not an essential aspect of the reduced dimensionality model used here, the role of tunneling is not discussed further in this paper. The relationship of this reduced dimensionality direct dynamical model to more traditional chemical theories, e.g., transition state theory, as well as a more detailed discussion of tunneling and the kinetic isotope effect will be presented elsewhere.[8]

A. PES

The PES utilized previously[2] has principally an entrance channel barrier and does not account for the very strong dependence of S_0 on T_v observed in Paper I. (Calculations based on this PES have more than an order of magnitude smaller dependence on T_v than is observed.) In addition, *ab initio* cluster calculations for CH_4 dissociation on Ni(111)[9,10] suggest that the transition state for that system occurs when a single C–H bond is extended by ca. 1. a.u., considerably more than in the original PES of Luntz and Harris. In order for the dynamical calculations to be qualitatively consistent with the cluster calculations for dissociation on a Ni surface, we have therefore constructed a two dimensional stiff lattice PES $V(Z,D)$ where the barrier is principally in the exit channel:

$$V(Z,D)=\tfrac{1}{2}[V_A+V_M-\sqrt{(V_A-V_M)^2+\chi^2}], \tag{1}$$

where $\chi=0.5$ eV is a mixing parameter, V_A and V_M are atomic and molecular potentials, respectively. V_A is almost identical to that used previously,

$$V_A=M[W_{\rm H},D_{\rm H},\lambda_{\rm H},(Z-0.5D)]+M[W_{\rm R},D_{\rm R},\lambda_{\rm R},Z] + V_{\rm RH}e^{-\lambda_{\rm RH}D}, \tag{2}$$

where the Morse function M is given as

$$M[W,X_0,\lambda,X]=W[1+F(F-2)]; \quad F=e^{-\lambda(X-X_0)}. \tag{3}$$

Specific parameters for V_A are $W_{\rm H}=2.76$ eV, $\lambda_{\rm H}=0.53$ a.u.$^{-1}$, $D_{\rm H}=1.1$ a.u., $W_{\rm R}=2.17$ eV, $\lambda_{\rm R}=0.7$ a.u.$^{-1}$, $D_{\rm R}=3.4$ a.u., $V_{\rm RH}=100$ eV, and $\lambda_{\rm RH}=1.6$ a.u.$^{-1}$ However, V_M is modified from before and is given as

$$V_M=W_mF[F-\gamma(Z)]-V_{\rm min}(Z)+V_0e^{-\lambda_0Z}, \tag{4}$$

with $F=e^{-\lambda_m(D-D_m)}$ and the attractive term $\gamma(Z)$ given as

$$\gamma(Z)=(2-\eta)+\eta\tanh[(Z-Z_c)/W_Z]. \tag{5}$$

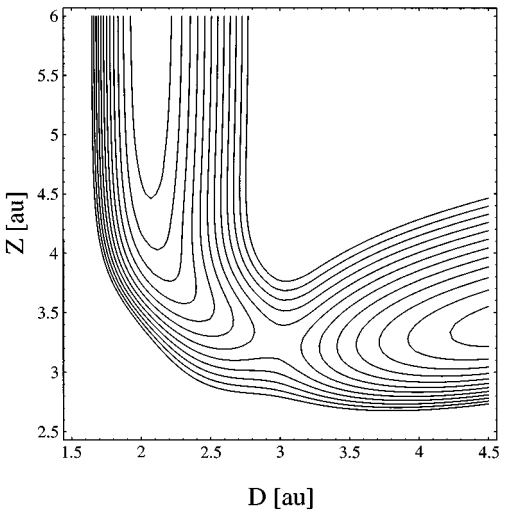

FIG. 1. Contour plot of the stiff lattice PES $V(Z,D)$ used in the model. Z and D are given in a.u. and the energy contour interval is 0.1 eV.

The Z dependent well depth $V_{\rm min}(Z)$ is given by

$$V_{\rm min}(Z)=W_mF_2(Z)[F_2(Z)-\gamma(Z)], \tag{6}$$

where $F_2(Z)=e^{-\lambda_m[D_{\rm min}(Z)-D_m]}$ and the Z dependent equilibrium bond length $D_{\rm min}$ is given as $D_{\rm min}(Z)=\ln[2e^{\lambda_mD_m/\gamma(Z)}]/\lambda_m$. For $\gamma(Z)\equiv 2(\eta=0)$, V_M is again a simple Morse potential plus an exponentially repulsive term. However, we use the parameters $\eta=0.5$, $Z_c=3.5$ a.u., and $W_Z=0.5$ a.u. which corresponds to a Morse-like potential but with a variable attractive term which depends on Z. Other parameters in V_M are $W_m=4.87$ eV, $\lambda_m=0.97$ a.u.$^{-1}$, $D_m=2.06$ a.u., $V_0=90$ eV, and $\lambda_0=1.5$ a.u.$^{-1}$

This PES is similar in spirit to that originally presented by Luntz and Harris, e.g., the PES is constructed from a Landau–Zenner mixing of an atomic potential V_A and molecular potential V_M. The chief difference to the PES used previously is that the well depth in V_M is weakened and the equilibrium bond length stretched in a smooth fashion as the molecule approaches the surface. Both effects are appropriate to describe the filling of a molecular antibonding resonance as the molecule approaches the surface, which is the essential physics underlying an exit channel barrier. Parameters were chosen to position the barrier at $D\approx 3$ a.u., in agreement with the cluster calculations, and to reproduce the barrier height V^* used previously by Luntz and Harris. The latter is strictly for convenience in comparing to dynamical calculations on the previous (entrance channel) PES,[2] but is certainly qualitatively consistent with estimates of V^*.[9,10] Other than these initial considerations, no further attempt was made to adjust the PES to optimize agreement of the dynamical calculation with experiment. A contour diagram of the PES $V(Z,D)$ is shown in Fig. 1.

The fundamental reason that the barrier in the PES for dissociation on Ni may be further towards the exit channel relative to that for Pt cannot be answered unequivocably until electron structure calculations are performed for CH_4 interacting with Pt (clusters or supercell). One possibility, however, is the suggestion that dissociation on Pt is slightly endothermic.[7] Such endothermicity usually pushes the barrier towards the entrance channel. Another possibility is that

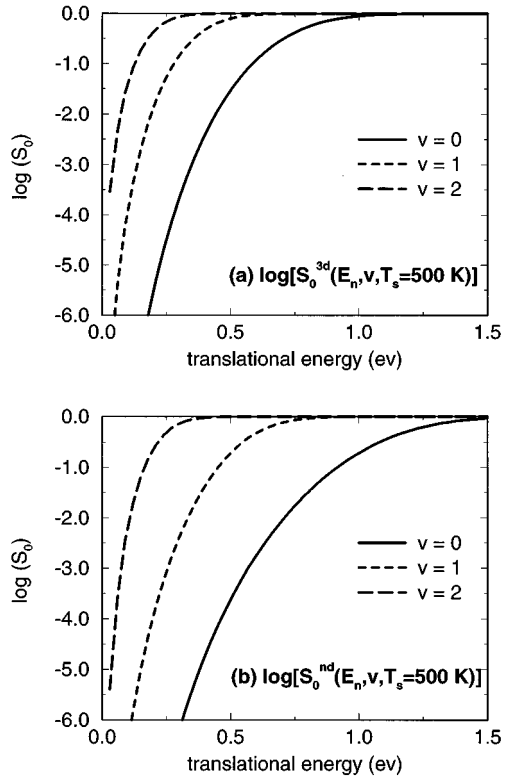

FIG. 2. Comparison of $S_0(E_n,v,T_s)$ for $T_s=500$ K calculated using the reduced dimensionality 3d model (a) with calculations using a multidimensional (nd) model (b).

since the Pt $5s$ orbital tails much further into the vacuum than the Ni $4s$ orbital (relative to the respective d orbitals), this should result in stronger Pauli repulsion for Pt (at large Z) and could shift the barrier towards the entrance channel.

The three dimensional PES $V_{3d}(Z,D,Y)$ is constructed in the same manner as before from the two dimensional PES,[2] i.e., $V_{3d}(Z,D,Y)=V(Z-Y,D)+(1/2)\kappa Y^2$. This describes the coupling of the barrier to the lattice and the bare phonon potential.

B. Three dimensional dynamics

The dynamics on the PES V_{3d} was calculated using the so-called surface mass model of Luntz and Harris. This model treats the molecular dissociation coordinates fully quantum mechanically but treats the phonon coordinate semiclassically. Details of the model and calculational methods were presented earlier. Values of $S_0^{3d}(E_n,v,T_s)$ are calculated for the three dimensional PES, where v is the R–H vibrational quantum number. An example is shown in Fig. 2(a) for $T_s=500$ K.

C. Multidimensionality: "Hole" model

The experimental results represent sticking in a multidimensional world and reflect much steric hindering. In Luntz and Harris this multidimensionality was not specifically included in the calculations, and its neglect was cited as the prime reason that the calculated increase in S_0 with incident energy was much faster than that of experiments; i.e., that the energy scale for all theoretical plots was roughly half that of the experimental plots. In this section, we approximately include the multidimensionality through the so-called hole model.[3,4] This model accounts qualitatively for the multidimensionality by relating the sticking to the (normalized) volume of phase space for which the incident energy is above the classical threshold. This represents a classical sudden approximation for the remaining $n-3$ dimensional coordinates, and accounts in an approximate way for the static distribution of barrier heights representing steric hindering. This neglects entirely, however, any dynamic coupling of these $n-3$ dimensional coordinates to the reaction path.

To incorporate these effects, we take the n-dimensional barrier height V_{nd}^* as

$$V_{nd}^*=V_{3d}^*+\Delta V^*, \tag{7}$$

where V_{3d}^* is the barrier height along the minimum energy path in Fig. 1 and ΔV^* represents the increase in barrier from steric hindering due to less than optimal impact parameters or orientational angles. For lack of any more definitive information, we simply assume that ΔV^* is distributed according to a Gaussian, $f(\Delta V^*)=e^{-(\Delta V^*-\Delta_0)^2/W^2}$. We choose $\Delta_0=0.4$ eV and $W=0.2$ eV to insure a gradual turn on of barriers generally consistent with the experimental widths observed in Paper I, as well as many other experimental systems. We do not, however, try to vary these parameters to achieve any specific fit to the data. Given this distribution of barriers, then the n-dimensional sticking $S_0^{nd}(E_n,v,T_s)$ is given according to the hole model as

$$S_0^{nd}(E_n,v,T_s)=\frac{\int S_0^{3d}(E_n-\alpha_v\Delta V^*,v,T_s)f(\Delta V^*)d(\Delta V^*)}{\int f(\Delta V^*)d(\Delta V^*)}, \tag{8}$$

where α_v represents the rigid shift of the sticking curve in the vth vibrational state with barrier shift ΔV^*. A reasonable approximation is $\alpha_v\approx d[\epsilon_c(v)]/d[\Delta V^*]$, with $\epsilon_c(v)$ the classical threshold for the given vibrational state obtained via two dimensional classical dynamics on the given PES. Values of α_v for the PES in Fig. 1 were determined by varying slightly one of the parameters (V_{RH}) which strongly affects principally the barrier height and then calculating the shift in the sharp classical thresholds for each vibrational state on the modified PES. $\alpha_v=1$, 0.5, and 0.1 for $v=0$, 1, and 2, respectively, on the PES of Fig. 1. $S_0^{nd}(E_n,v,T_s)$ for $T_s=500$ K is shown in Fig. 2(b). Comparison with $S_0^{3d}(E_n,v,T_s)$ of Fig. 2(a) shows that the multidimensionality broadens and lowers the sticking curves for each vibrational state, and that this effect is much more pronounced for the lower vibrational states due to the larger values of α_v. Because of this, a fit of these S_0^{nd} curves to simple S-shaped functions then produces vibrationally dependent thresholds which are separated by more than ω_{vib}. Thus the "inconsistency" in the fit of experimental S curves that is observed in Paper I is in fact a natural and necessary consequence of interpreting a multidimensional dissociation in terms of 2d (or 3d) dynamical models.

Sticking curves representing the various experiments in Paper I are then calculated via appropriate averages, i.e.,

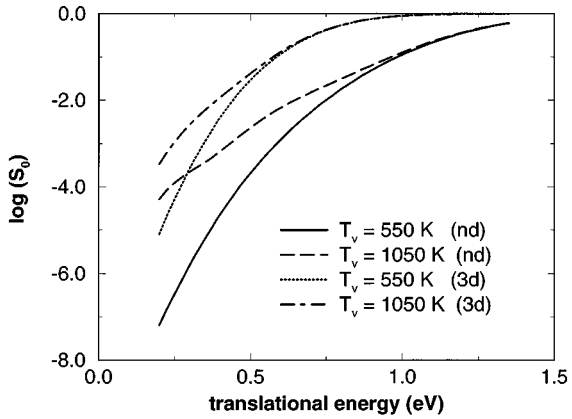

FIG. 3. A comparison of $S_0(E_n,T_v,T_s)$ at $T_v=550$ and 1050 K for $T_s=500$ K calculated using both the 3d and multidimensional (nd) models.

$$S_0(E_n,T_v,T_s)=\sum_v P_v S_0^{nd}(E_n,v,T_s) \tag{9}$$

with the vibrational population

$$P_v=g_v \exp-(v\omega_{\rm vib}/k_BT_v)/Q$$

with degeneracy factors $g_v=1$, 4, and 4 for $v=0$, 1, and 2, respectively, and Q is the normalizing factor. These values for g_v are necessary to correct for the fact that CH_4 has four equivalent C–H bonds rather than the one bond in the quasidiatomic model. In a related manner,

$$S_0(T_g,T_s)=\frac{1}{k_BT_g}\int_0^\infty dE_n\, e^{-E_n/k_BT_g} S_0^{nd}(E_n,T_v=T_g,T_s). \tag{10}$$

Figure 3 illustrates further the dynamic consequences of the multidimensionality in the PES by comparing $S_0[E_n,T_v=500$ K(1050 K), $T_s=500$ K] calculated using $S_0^{nd}(E_n,T_v,T_s)$ [Eq. (9)] with an analogous expression but using $S_0^{3d}(E_n,T_v,T_s)$. Thus in addition to lowering the overall magnitude of the sticking, the multidimensionality also stretches the energy scale and *enhances the role of vibrational excitation (T_v) relative to that of a 3d model using the same PES*. The latter occurs due to the much larger suppression of sticking in the lower vibrational states relative to the higher ones with the inclusion of steric hindering.

III. COMPARISON OF MODEL TO EXPERIMENTAL RESULTS

Figure 4 compares calculated values of $S_0^{nd}(E_n,T_v,T_s)$ with the measurements in Paper I. It is evident that there is excellent qualitative agreement, although the calculated dependence of S_0 on T_v is slightly less than that observed. No attempt was made to either vary the PES of Fig. 1 or the parameters defining $f(\Delta V^*)$ to improve the agreement since it is felt that this level of agreement is already beyond the limits of validity of approximations in the model.

Figure 5 compares the calculated isotope effect with that measured in Paper I. Again, excellent qualitative agreement is obtained. This isotope effect is principally determined by

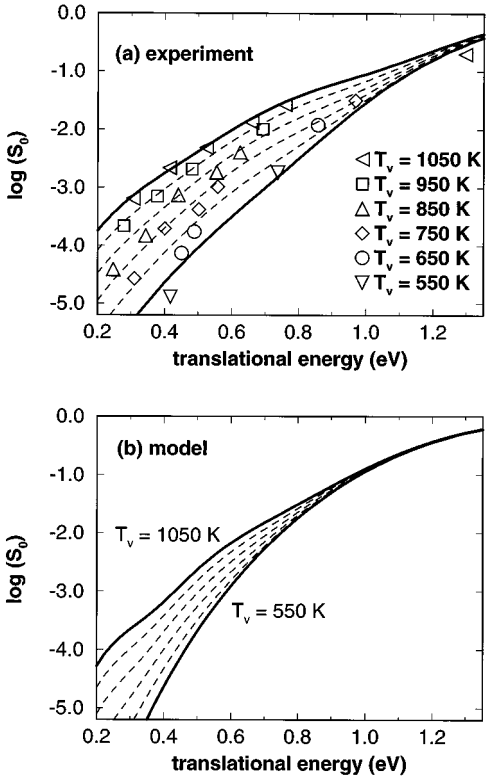

FIG. 4. Comparison of (a) experimental measurements of $S_0(E_n,T_v,T_s=475$ K) from Paper I with (b) calculations based on the nd model. The limiting T_v ranges, 550 and 1050 K are solid lines. Intermediate T_v (650, 750, 850, and 950 K) are dashed lines. The lines in (a) are from the experimentally derived S curves resulting from a fit to the experimental points. The experimental points in (a) are the measurements deconvoluted over the beam energy distribution.

the shift in vibrational zero point of R–D relative to R–H. The fact that the calculated isotope dependence is slightly less than that observed is in complete accord with the slightly smaller role of T_v in S_0 exhibited in Fig. 4.

Figure 6 compares the calculated T_s dependence with that observed in Paper I. Again, good qualitative agreement is obtained. For the experimental conditions prevailing in Paper I, the observed T_s dependence is rather modest in Fig. 6(a). This T_s dependence does, however, become stronger as E_n and/or T_v are lowered. Both effects are apparent in model calculations. In fact, at both low T_v ($\ll$450 K) and E_n, the T_s dependence is predicted to be quite strong. This region is unfortunately not experimentally accessible since S_0 is too low to measure for these conditions. The reason the T_s dependence is so small at $T_v=850$ K is that the S_0 is then dominated by sticking of the higher vibrational states where the sticking is large and the center of mass energy dependence due to surface thermal motion is slight. It should be pointed out that the model calculations for the increase in the T_s dependence at lower T_v preceded the experiments, so that this represented a prediction of the model.

Figure 7 compares the calculated isothermal ''bulb'' dissociation probability with both experiment[11] and S_0 calculated using extrapolations of the experimentally derived S

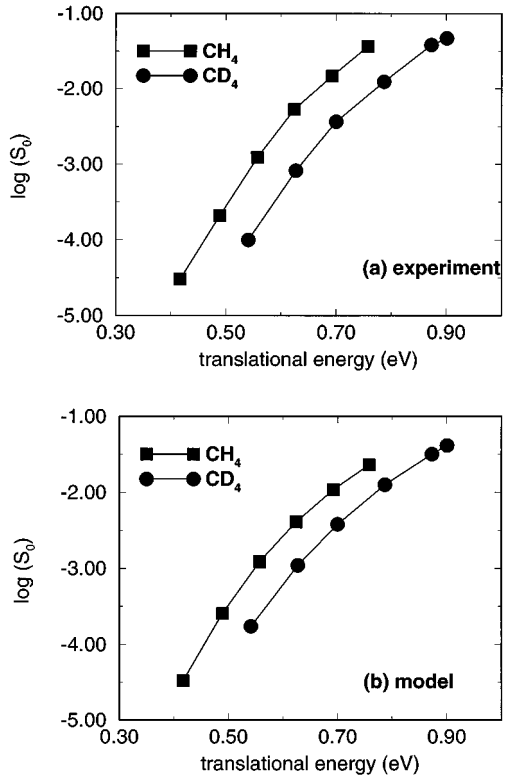

FIG. 5. Comparison of the measured isotope effect in Paper I (a) with that calculated using the *nd* model (b). $T_s = 475$ K for all measurements, but various T_v were utilized (see Paper I). Conditions were duplicated for all calculations in (b).

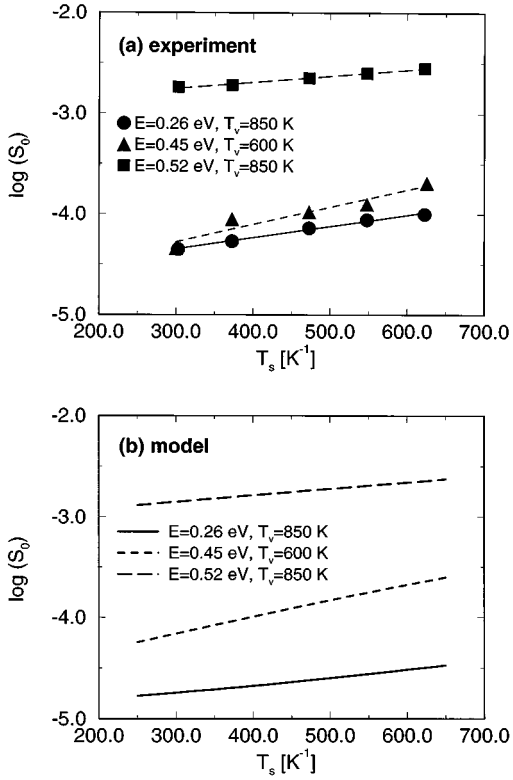

FIG. 6. Comparison of the experimental dependence of $S_0(E_n, T_v, T_s)$ on T_s for different E_n and T_v from Paper I (a) with that calculated using the *nd* model under identical conditions (b).

curves of Paper I. As stressed in Paper I, there is excellent agreement between the thermal rates and predictions based purely on the molecular beam experiments (experimentally derived *S* curves). This was taken as partial evidence that the same direct dissociation mechanism that dominates the beam experiments is also dominant in the bulb experiments. We see that there is also excellent agreement of the thermal rates with the direct dynamical model as well, further confirming this conclusion. Both the molecular beam experiments and the model predict some curvature in a plot of log (S_0) vs $1/T$ over an extended temperature range, e.g., non-Arrhenius behavior. This arises principally from the varying dominance of different (quasidiatomic) vibrational states in the temperature range and their different overall dependence on T. The model predicts a somewhat higher T (750 K) than the experimental *S* curves (300 K) for the dominance of vibrationally excited states in the isothermal rate, in general agreement with the somewhat smaller effects of T_v in the model (Fig. 4). Nevertheless, the curvature in both results imply that there should also be some experimental curvature as well if measurements were possible over such an extended temperature range. This suggests that there is some additional uncertainty in estimating the rate in the catalytically important temperature range of ca. 1000 K from a pure Arrhenius extrapolation of rates measured at lower T. In addition, calculated apparent activation energies, i.e., slopes in the plot of log (S_0) vs $1/T$, vary considerably over the range of T and only at very high T ($\geqslant$1000 K) become equivalent to the potential barrier height of 0.76 eV assumed in the model. The fact that such Arrhenius plots often do not measure true barrier heights has been stressed previously.[2,6] At isothermal conditions ($T_g = T_s$) and at sufficiently high T (or wide barriers) so that tunneling is completely unimportant, then traditional transition state theory may provide an approximation to the isothermal rate of reaction for this mechanism of direct dissociation. Naturally transition state theory can say nothing about the molecular beam experiments under nonequilibrium initial conditions.

In addition to the direct mechanism discussed here, other authors have suggested that the dissociation of CH_4 on metals is dominated by completely different mechanisms. For example, Ukraintsev and Harrison[12] have proposed a statistical mechanism for dissociation where the CH_4 is strongly coupled to a local cluster of surface atoms. This strongly coupled collision complex subsequently decays via RRKM unimolecular decay. With several adjustable parameters, a model of this mechanism has produced reasonable fits to molecular beam experiments on another system [Pt(111)]. A fit of this statistical model to the experiments reported in Paper I may also be possible. However, ''fits'' of a model to experiments should not be taken as irrefutable proof of the mechanism. Hence, the detailed agreement obtained by fits of either the direct dynamical model or the statistical model with experimental results should be viewed quite cautiously. However, the direct dynamics mechanism and the RRKM unimolecular decay mechanism are based on completely different physics so that they should *predict* quite different be-

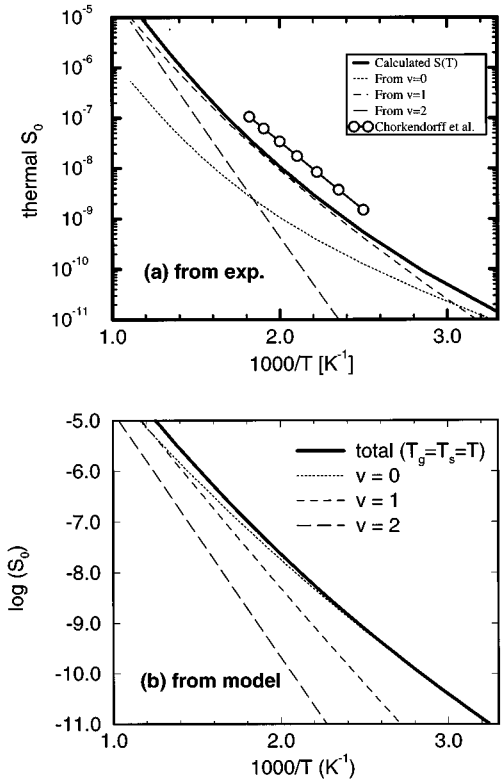

FIG. 7. Comparison of the isothermal rate measured previously and as predicted from the experimentally derived S curves of Paper I (a) with $S_0(T_g=T_s, T_s)$ calculated using the nd model (b). The solid line is the total rate and the various dashed curves are the contributions of individual vibrational states to the overall thermal rate.

haviors for future experiments that are specifically designed to distinguish between mechanisms. Naturally, this author feels that the direct mechanism provides the most reasonable physical basis for a description of the dissociation process.

IV. CONCLUSIONS

It is suggested in Paper I that the experimental molecular beam results are consistent with a mechanism of direct dissociation on a PES with an exit channel barrier. In this paper, a detailed comparison is presented for the predictions of a quantum dynamical model for such a mechanism with the experimental results of Paper I. The experimental results are only partially consistent with a reduced dimensionality (3d) model since the experiment requires vibrationally dependent S curves which are separated by more than ω_{vib}. Inclusion of multidimensionality (steric hindering) via the hole model, however, produces excellent agreement with the experiments and removes any inconsistencies. The overall good agreement between the model and the experiment demonstrates that the mechanistic conclusions of Paper I are at least justifiable and reasonable.

There has been no attempt in the model to fit the experimental data. A reasonable PES and barrier distribution have been simply assumed at the outset without any reference to the experimental data of the previous paper. Even better agreement between the model and experiment could be easily achieved by ''adjusting'' the width of the barrier distribution in the hole model (and perhaps the PES). However, the level of agreement between the model calculations and experiment is already felt to be better than the limitations imposed by the approximations in the model, so that ''fitting'' the data by adjusting such parameters would be misleading as to the accuracy of such a model.

ACKNOWLEDGMENTS

The author gratefully acknowledges the Danish Research Academy for supporting this work, and thanks many members of the Physics Department of the DTU for their hospitality and help while this work was performed.

[1] P. M. Holmblad, J. Wambach, and I. Chorkendorff, J. Chem. Phys. **102**, 8255 (1995).
[2] A. C. Luntz and J. Harris, Surf. Sci. **258**, 397 (1991).
[3] M. Karikorpi, S. Holloway, N. Henriksen, and J. K. Norskov, Surf. Sci. **179**, L41 (1987).
[4] K. Gundersen, K. Jacobsen, J. K. Norskov, and B. Hammer, Surf. Sci. **304**, 131 (1994).
[5] J. Harris, J. Simon, A. C. Luntz, C. B. Mullins, and C. T. Rettner, Phys. Rev. Lett. **67**, 652 (1991).
[6] A. C. Luntz and J. Harris, J. Vac. Sci. Technol. A **10**, 2292 (1992).
[7] A. C. Luntz and H. Winters, J. Chem. Phys. **101**, 10980 (1994).
[8] A. C. Luntz (to be published).
[9] H. Yang and J. L. Whitten, J. Chem. Phys. **96**, 5529 (1992).
[10] H. Burghgraef, A. P. J. Jansen, and R. A. van Santen, Chem. Phys. **177**, 407 (1993).
[11] I. Chorkendorff, I. Alstrup, and S. Ullmann, Surf. Sci. **227**, 291 (1990).
[12] V. A. Ukraintsev and I. Harrison, J. Chem. Phys. **101**, 1564 (1994).